A wireless cloud network platform for industrial process automation: critical data publishing and distributed sensing

Leonardo Ascorti, Stefano Savazzi, Gloria Soatti, Monica Nicoli, Emiliano Sisinni, Stefano Galimberti

***Abstract*—Wireless technologies combined with advanced computing are changing industrial communications. Industrial wireless networks can improve the monitoring and the control of the entire system by jointly exploiting massively-interacting communication and distributed computing paradigms. In this paper, we develop a wireless cloud platform for supporting critical data publishing and distributed sensing of the surrounding environment. The cloud system is designed as a self-contained network that interacts with devices exploiting the Time Synchronized Channel Hopping protocol (TSCH), supported by WirelessHART (IEC 62591). The cloud platform augments industry-standard networking functions as it handles the delivery (or publishing) of latency and throughput-critical data by implementing a cooperative-multihop forwarding scheme. In addition, it supports distributed sensing functions through consensus-based algorithms. Experimental activities are presented to show the feasibility of the approach in two real industrial plant sites representative of typical indoor and outdoor environments. Validation of cooperative forwarding schemes shows substantial improvements compared with standard industrial solutions. Distributed sensing functions are developed to enable the autonomous identification of recurring co-channel interference patterns.**

***Index Terms*—Industrial wireless sensor networks, dense cloud networks, sensor-cloud networking, cooperative communication, consensus-based distributed estimation, interference detection, industrial Internet of Things.**

I. Introduction

Industrial automation applications have greatly changed in the last years, growing in size and complexity. Nowadays, industrial devices such as measuring instruments, Programmable Logic Controllers (PLCs) and Industrial PCs running Supervisory Control and Data Acquisition (SCADA) systems embed powerful logic capabilities that allow for high adaptability, modifying their behavior depending on the sensed surrounding environment and on interactions with other devices. The need for better control of the process and an increased production efficiency push these evolutions, in order to increase the overall performance. A large base of interconnected systems employing machine-to-machine communications for process automation and/or monitoring thus provides a better knowledge of what is happening in the plant, augments its flexibility and manageability, and discloses the opportunity to deploy augmented services [1].

Recently, two disruptive technologies as part of the industrial Internet of Things (iIoT) paradigm gained popularity in the process automation world, i.e., Industrial Wireless Sensor Networks (IWSNs) and cloud computing. Wireless communications are adopted at the field level, implementing wireless counterpart of typical field-buses. Purposely tailored standards appeared to satisfy the requirements of process automation and/or monitoring in terms of timeliness and reliability. The Time Slotted Channel Hopping (TSCH) medium access is a popular solution facilitating energy-efficient mesh/multi-hop communications, while reducing fading and interference impairments. This policy is supported by the WirelessHART or the ISA100.11a solutions, formally known as IEC 62591 and IEC 62734 standards [2]. Cloud computing has been suggested as a tool for providing different kinds of services for the industrial automation: a recurrent expression is “X as a Service”, where usually X can be Software, Platform or Infrastructure [3], [4]. Only recently wireless sensor networks and cloud paradigm have been merged into a single entity, sometimes addressed as sensor-cloud infrastructure [5], [6].

This work is a step ahead in the direction of industrial cloud platform design. In industrial environments the equipment lifetime should be considerably long (between 10 and 15 years). For this reason, solutions that guarantee compatibility with existing standards and augment/extend their functions when needed are truly indispensable [7], [8]. In line with this trend, the proposed architecture mixes the advantages of both IWSNs and cloud paradigms: as depicted in Fig. 1, it consists of a self-contained network specifically designed to operate in parallel with an existing IWSN (IEC 62591 - WirelessHART compliant) to augment its baseline networking and sensing functions on on-demand basis. The cloud network

This work has been performed in the framework of the EU research project DIWINE - Dense Cooperative Wireless Cloud Network - under FP7 ICT Objective 1.1 - The Network of the Future. It has been partially funded by project ESPOL - Smart Refinery: Wireless Network Deployment Study in PetroEcuador Esmeraldas DIT.AD003.057, and CNR-ESPOL Memorandum de Acuerdo Interinstitucional CNR-IEIIT and ESPOL, Oct. 2015. L. Ascorti and S. Galimberti are with Pepperl+Fuchs srl, Sulbiate (MB), Italy. S. Savazzi is with Consiglio Nazionale delle Ricerche (CNR), Institute of Electronics, Computer and Telecommunication Engineering (IEIIT) Milano, Italy (e-mail: stefano.savazzi@ieiit.cnr.it). G. Soatti and M. Nicoli are with the Dipartimento di Elettronica, Informazione e Bioingegneria (DEIB), Politecnico di Milano, Milano, Italy (e-mail: gloria.soatti@polimi.it; monica.nicoli@polimi.it). E. Sisinni is with the Department of Information Engineering, University of Brescia, Brescia, Italy (email: emiliano.sisinni@unibs.it). The work has been partially presented at IEEE Sensors and Applications Symposium (SAS), Catania, Italy, April 2016.

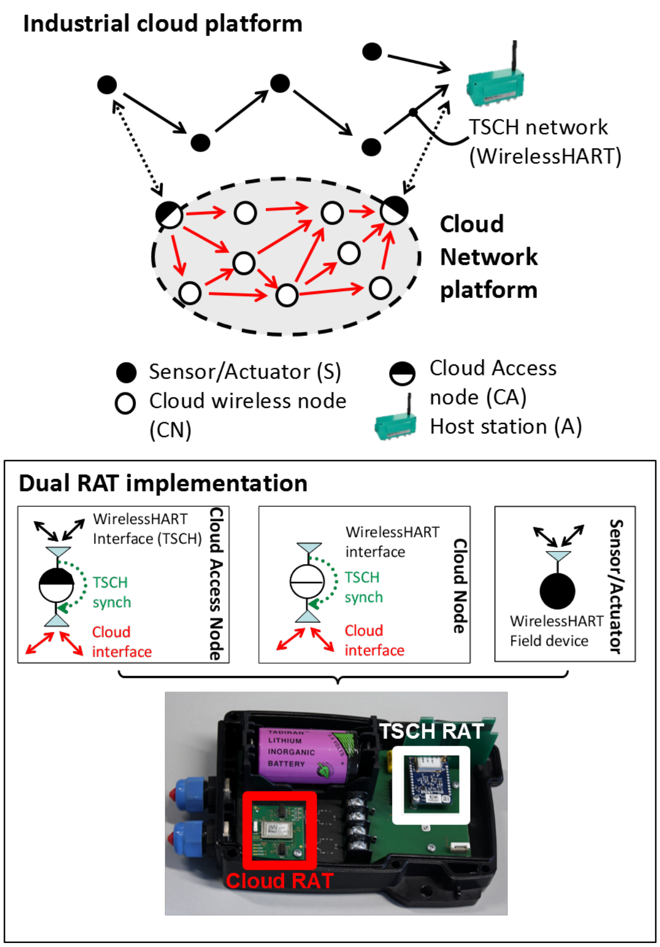

Fig. 1. Industrial wireless sensor network architecture and field-level cloud platform. Bottom: dual radio-access technology (RAT) implementation (layered network architecture); P+F battery-powered cloud node prototype supporting dual RAT.

adopts low-level cooperative communication technologies tailored for densely interconnected devices that are designed to support real-time and critical communication tasks, as well as distributed computing services.

The paper is organized as follows. Sect. II introduces the cloud platform as well as it highlights the background, main contributions (Sect. II-A) and proposed approach (Sect. II-B). The implementation of the wireless interface, the related cooperative networking and the distributed computing algorithms are detailed in Sect. III. Validation of the cloud functions is carried out in two representative industrial sites detailed in Sect. IV. The problem of critical data publishing is addressed in Sect. V by extensive experimental studies and comparative analysis with TSCH standard solutions. Next, distributed sensing and computing functions are demonstrated in Sect. VI to enable the autonomous learning of recurring interference patterns as critical in shared spectrum access scenarios.

II. Cloud Architecture

Industrial wireless communication technologies take advantage of cable removal and higher scalability/flexibility of the wireless connectivity, to increase the plant status knowledge thanks to a large number of installed field devices [8]. At the same time, cloud computing is emerging as the future computing paradigm, enabling on-demand access to a shared pool of configurable computing resources [9], including the underlying communication infrastructure. Up to now, these two technologies, i.e., communication and computing, have been operating independently, at different level of the automation pyramid. Very few efforts have been carried out in order to match the cloud paradigm with the requirements of an industrial network [10].

A. Background and contributions

Off-the-shelf IWSN technologies support long-term deployments while industry-standard protocols are primarily designed to be energy efficient [11], [12] and optimized to handle periodic or non-critical traffic [13]. On the other hand, current trends in industrial automation (i.e., Industry 4.0) are pushing towards the transformation of factories into flexible production systems, where wireless technologies will play a crucial role only if paired with advanced solutions to support time-critical and highly reliable applications demanding for prioritized traffic and/or strict real-time constraints. Therefore, to allow for wider adoption of wireless networks in an industrial context, substantial technology innovation is required in terms of new types of devices supporting decentralized functions, self-configuring and learning protocols, communication and computing strategies to support delay/safety-critical applications. Although the majority of existing wireless network designs consider energy consumption, recently some works focused on delay and reliability optimization that are essential to support mission-critical applications (see [13] and references therein). For example, priority-enhanced MAC protocols, mostly designed for delay-critical traffic have been developed in [14], [15]. In general, these protocols provide service differentiation for traffic categories characterized by increasing criticality. Although experimental validations [14] and simulation-based comparative analysis [15] confirm the potential of these emerging solutions, their practical deployment to replace an existing industrial network has never been addressed. In fact, these solution are not designed to coexist with current industrial products, as they rely on a complete redefinition of the low-level MAC structure. On the contrary, the proposed system exploits a cloud platform that validates the integration of advanced networking and computing functions with an industry-standard IWSN implementation (IEC 62591). The approach presented in the paper is one of the few trying to merge the “Hardware/Infrastructure as a Service” (H/IaaS) and “Platform as a Service” (PaaS) models with IWSNs. For example, the proposed cooperative wireless network infrastructure is a step towards the network level virtualization [16], where the peculiar characteristics of industrial wireless communications pose additional requests, which cannot be easily solved using legacy technologies. Indeed, the goal of the work is to experimentally verify (in a real-world testbed) the performance that can be obtained implementing a I/PaaS approach using cloud devices specifically tailored as a complement to regular IWSN. The proposed solution thus guarantees coexistence and support any industry-standard wireless protocol stack that builds on the IEEE 802.15.4e TSCH mode. Differently from previous proposals [9], [5], the cloud nodes are designed to augment conventional industrial network functions and they can lease extended services to pre-existing industrial equipment, upon request.

As described in the following sections, the advanced networking functions supported by the cloud originate from the emerging area of distributed cooperative communications [17]. The cooperative link abstraction generally consists of separate radios encoding/transmitting or decoding/receiving messages in coordination [18]. Information theoretic (see, e.g., [19] and references therein) as well as experimental validations in confined environments [20] showed that those systems could achieve enhanced reliability compared to standard solutions as mimicking the performance of a wired system. Despite some recent attempts to develop cooperative relaying features tailored to IEEE 802.15.4 sensor networks [21][22], practical methods to integrate such schemes into a fully fledged industrial standard are still missing.

Cooperative networking as supported by the cloud platform also enables to implement decentralized sensing, processing and estimation tasks by means of consensus algorithms. Distributed consensus-based techniques allow the network to self-learn its own state and self-organize without the support of any central aggregation unit, also in critical dynamic scenarios, facilitating energy-efficient, high-throughput and low-latency network communications [11]. In contrast with the "Host-centric" structure of current IWSNs, the use of consensus strategies algorithms allows to implement "device-centric" estimation tasks which exploit decentralized intelligence at the cloud node side. In the recent literature, consensus methods have been investigated for a number of distributed estimation applications, including channel estimation [23], network synchronization [24], localization [25] and interference sensing [26]. In [27] and [28], they have been employed in a sensor network hardware platform aiming at optimizing the sensor energy consumption. These strategies look therefore promising for integration into an industrial standard. In this context, this paper shows for the first time the exploitation of such algorithms in a real industrial plant monitoring platform for autonomous identification of recurring interference patterns in a shared spectrum.

B. The proposed approach

As previously stated, research works on sensor-cloud networking did not address real-time needs, since most of existing infrastructures [4] relax timing constraints in order to allow the execution of complex tasks, e.g., related to sensor (and actuator) abstraction. On the other hand, as depicted in Fig. 1, the proposed system combines communication and computing technologies into a dense, self-contained cloud of wireless interconnected nodes (cloud nodes, CNs). These nodes cooperate at physical (PHY) and medium access control (MAC) layer [29] to provide seamless communications and distributed sensing/processing services to an IWSN referred to as "TSCH network", as conforming to the TSCH mode (WirelessHART standard). In the example of Fig. 1, messages (datagrams/data-frames), originating from the sensor/actuator field devices or the Host station serving as IWSN manager, can be off-loaded through the cloud network. The cloud consists of nodes (CNs) cooperating directly at PHY/MAC to create a powerful "virtual" relay/processing unit that supports both critical data forwarding and distributed processing tasks. The platform operates at field level and it is designed as both H/IaaS and PaaS service provider. It can lease a network infrastructure and physical-layer resources (e.g., communication functions) to effectively manage on-demand critical data publishing services through the implementation of cooperative communication policies [17], [19]. In addition, it delivers a computing platform that allows to deploy and run decentralized estimation tasks through consensus algorithms [30], [23] implemented internally inside the cloud. Distributed estimation is accomplished by means of a novel distributed weighted-consensus strategy that reduces the signaling between nodes and guarantees at the same time fast convergence to the equivalent centralized sensing that would be accomplished by a virtual Host fusing and processing all the data collected in the cloud.

The Host station, acting as sink node and network manager for the TSCH network, does not manage or control the underlying cloud hardware infrastructure, but has control over the traffic offloading and the computing tasks, depending on the deployed instrumentation. The execution of these tasks can be dynamically planned by the Host station based on end-user requirements. To this end, the cloud access (CA) nodes are specific devices designed to act as distributed cloud controllers and provide a uniform PHY/MAC interface (TSCH-compliant) to both Host and industrial field devices requesting for cloud services. All the communication and distributed estimation tasks are thus performed within the cloud network, so that field devices at the edge are blind to the inner workings of the cloud.

III. Implemented platform and algorithms

The test-bed system consists of industrially compliant wireless field devices under-laid with a distributed and self-contained network consisting of nodes (CNs) and cloud access points (CAs). Prototype and implementation are summarized in Fig. 1 at bottom. Cloud nodes are battery-powered and equipped with a dual radio access technology (RAT). The first radio supports the industry standard TSCH mode conforming with IEC 62591 (WirelessHART). It is primarily intended to synchronize the cloud network to the reference clock provided

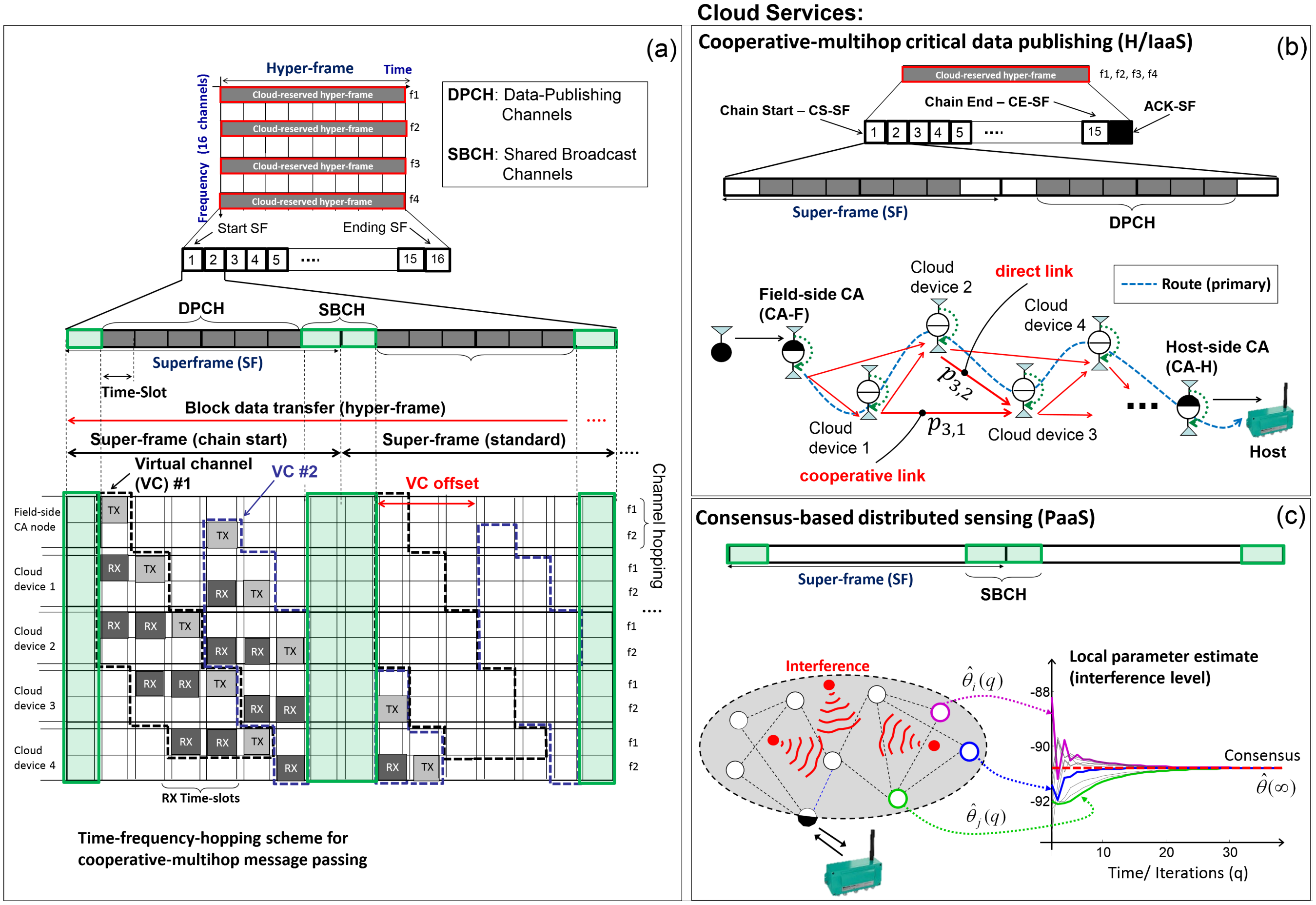

Fig. 2. Cloud architecture (a): TSCH based framing structure (super-frames, hyper-frames, DPCH and SBCH channels), virtual channels (VCs) and frequency hopping patterns. (b) Cooperative-multihop message passing, chain-start, chain-end and ACK superframes. (c) Distributed estimation of the network-state parameters θ (e.g., interferer received signal strength level) throughout cooperation between the CNs.

by the Host station, which controls industrial monitoring functions. The second radio supports the cloud functions: it adopts an ad-hoc radio interface defined on top of the IEEE 802.15.4e PHY standard [2] and implements low-level (PHY/MAC) cooperative networking functions. The reference architecture for the identified dual-RAT solution thus entails two independent transceivers - with separate antennas - deployed inside each cloud device (including CNs and CA nodes) that are tightly coupled with a high-integration system-on-a-chip [31] to provide coordinated support to the MAC layers associated with both the TSCH-based and the cloud-based networks. This dual-layer model entails the loosely coupled coexistence between the IWSN protocol stack and the "cloud-oriented" layer that applies the cloud functions. The usage of two independent RF modules allows the cloud network to operate simultaneously with the pre-existing IWSN to augment its basic networking and sensing functions. It also simplifies the coexistence and the compatibility with the installed base at the price of a limited increase of the hardware costs. To allow for parallel network operation, the frequency channels allocated to the cloud are separated from those allocated to the TSCH network: the system can thus implement transmissions over non-contiguous frequency channels and better exploit frequency diversity. In addition, different data-rates (with varying direct-sequence spread spectrum - DSSS - options) are chosen for cloud device connectivity and optimized to manage the off-loaded traffic based on the specific environment.

A. Cloud interface and synchronization

As summarized in Fig. 2-(a), the communication among the CNs takes place over a series of contiguous, synchronized fixed-length slots of 10ms each, organized in super-frames of 8 slots and hyper-frames collecting 16 consecutive super-frames, relating to the same communication session. Every CN has a shared notion of time while the cloud system is able to keep the timing error below a maximum specified limit. A precise synchronization allows to enable an efficient distributed scheduled access of CNs as well as a reduced energy consumption. The baseline clock information is defined as the Cloud Network Time (CNT) and provides a timing reference (with resolution of microseconds) that is shared by all the CNs. The cloud radio interface exploits the TSCH layer to acquire the CNT information: in the proposed implementation this is directly derived from the absolute slot information (ASN) [32]. Considering that no standardized way is available to directly access the ASN information, the CN transceiver is designed to use the HART real-time clock command (CMD 90) through the wired communication interface connecting the two RAT interfaces inside each CN.

As introduced in Sect. II, the CA nodes provide an interface to industrial devices outside the cloud requesting for augmented services. Access nodes can be dynamically configured as 'host-side' cloud access nodes (CA-H) providing to the Host station an access point to the cloud, and 'field-side' cloud access nodes (CA-F) granting new requests from HART field devices. For example, in critical data publishing applications (see Fig. 2-(b)), the cloud makes possible a 'virtual' connection between a pair of CA nodes in a manner which is transparent (or invisible) to the nodes member of the underlying IWSN. In fact, thanks to the dual-RAT implementation, the CAs also act as field devices of the TSCH network and can thus seamlessly interact with the Host station being unaware of the embedded cloud processing. The cloud and TSCH radio interfaces inside each CA node communicate via a wired communication channel which – for uniformity reasons – is based on the HART Transport Layer format. In particular, the transceiver of the CA-H supporting the TSCH protocol acts as a master HART device for the cloud section, similarly as a WirelessHART adapter device [32]. On the contrary, the cloud transceiver of the CA-F node acts as a master HART device for the TSCH radio interface layer: communication between the two radio sections is based on the wired HART maintenance port, available within each standard-compliant HART device.

On every superframe, publishing of data originating from CA devices interfacing with the cloud is implemented over 6 contiguous channels (data publishing channels - DPCH - highlighted in grey in Fig. 2-(a)). A cooperative-multihop forwarding scheme [22] is engineered and adapted so as to leverage both spatial and temporal diversity [19] for point-to-point data transmission (Sect. III-B). The cooperative scheme is designed in order to (i) be robust to packet losses under high-throughput applications and (ii) meet stringent delay deadlines. Two shared broadcast channels (SBCH - highlighted in green) are also configured inside each superframe to propagate CA control/configuration functions as well as to implement decentralized sensing tasks (Sect. III-C).

B. Cooperative-multihop transmission chain system

A multi-hop chain of consecutive transmissions is developed to support point-to-point communication among a pair of CA nodes (field-side CA-F and Host side CA-H nodes, respectively), for the purpose of data publishing. A sequence of intermediate relaying CNs must first be defined (e.g., CNs 1-4 in Fig. 2-(b)). Once the chain is defined, possibly by layout optimization [10] or relay selection [33], [20], the field-side CA source node takes the datagrams on the TSCH radio interface and tunnels them through the cloud section. Each cloud node handles data forwarding by "duo-cast" mode (e.g., transmitting the same datagram/packet towards the two following nodes in the route path), up to when the host-side CA destination node is reached. Each packet always has two propagation opportunities – and similarly the destination node has always two packet receive opportunities, corresponding to a "cooperative diversity" order [19] of 2. The packet delivery rate $\mathrm{P}(n)$ observed at n-th cloud node along the multi-hop route $n = 1, 2, 3...$ can be therefore effectively approximated using the recursive expansion

$$\mathrm{P}(n) = (1 - p_{n,n-1})\mathrm{P}(n-1) + p_{n,n-1}(1 - p_{n,n-2})\mathrm{P}(n-2) \tag{1}$$

where $p_{n,n-1}$ indicates the observed packet drop probability for link between CN n and its closest neighbor $n-1$ (*direct link*) and similarly $p_{n,n-2}$ refers to the same probability now for the link between node n and its corresponding two-hop neighbor node $n-2$ (*cooperative link*), see the example in Fig. 2-(b) for CN 3.

The communication among the CNs takes place over consecutive DPCH slots. Within each slot, a single CN can thus transmit while selected CNs along the route path can receive in "multicast" mode. In order to allow for multicast operation, and differently from typical WirelessHART standard solutions, intra-slot acknowledgment is disabled along the multi-hop route. It can be observed that, although no intra-slot retry is performed, the cooperative multi-hop algorithm allows an "implicit-retry" capability resulting from its multiple packet propagation and receive opportunities.

Each data frame can be transmitted on a different IEEE 802.15.4 frequency channel: more than one node can therefore transmit within the same slot, providing that a different frequency channel is used. Resource allocation granularity is the Virtual Channel (VC) defined as a pseudo-random sequence of non-overlapping IEEE 802.15.4 channels carrying simultaneous data transfers through the cooperative-multihop chain. As depicted in Fig. 2-(a), in the current test-bed, two distinct VCs are allocated in each superframe with time offset of 30ms (VC offset), but this number could be configured depending on the number of channels allocated to the cloud platform. Consecutive VCs can be leased for data publishing to a requesting CA node and for a number of consecutive hyper-frames.

As detailed in Fig. 3, the chain system is designed to operate in two modes, namely: i) *datagram transmission mode*, where consecutive VCs are used to multiplex different datagrams; ii) *reliable transmission mode*, where the same datagram can be re-transmitted over a (configurable) number of consecutive VCs, corresponding to consecutive super-frames (or hyper-frames). Datagram transmission mode provides a high-throughput device-to-device data block transfer service, emulating a virtual communication bus where end-to-end retransmission is a viable option and for which the overall end-to-end throughput is the key performance indicator. Reliable transmission mode adds configurable redundancy in exchange for reduced throughput, it is therefore designed to provide

Framing structure

Cloud-reserved channels	f1=2405MHz, f2=2425MHz, f3=2445MHz, f4=2465MHz
Slot size	10ms
Super-frame (SF) size	8 slots (80ms)
Hyper-frame length *H*	*H*=16 SF (15 + ACK)

PHY data-rate	500Kbps	Throughput
Max. datagrams per hyper-frame *T*	*T*=29	Throughput
Frame payload *L*	*L*=80 bytes	Throughput
Virtual Channel offset	3 slots (30ms)	
Cooperative diversity factor	2	
Number of hops (per chain)	3 (typical), 6 (max.)	

Cooperative-multihop parameters

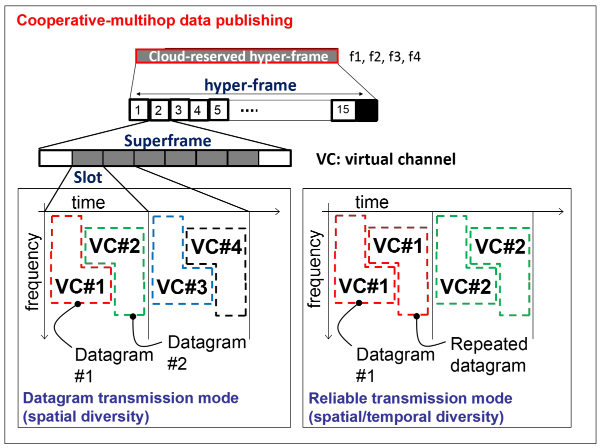

Fig. 3. Cooperative-multihop networking: main parameters for test-bed evaluation (top), datagram and reliable transmission modes (bottom).

an high reliable and low-latency end-to-end communication service for which reliability (packet drop rate, PDR) and latency are the key performance indicators. In the experimental tests of Sect. V, latency corresponds to the arrival time of the first packet of each hyper-frame received at the chain-end (see Fig. 2-(b)).

C. Consensus-algorithms for distributed sensing

In current TSCH implementations, network-state estimation and process monitoring are performed centrally by the Host station collecting observations from all field devices. In this section the use of the cloud platform is investigated to support a decentralized estimation/monitoring.

Distributed processing techniques enable the CNs to estimate the network-state parameters in a fully distributed way and self-organize without the support of any central coordinator. A crucial task in IWSN design is interference sensing in order to allocate the radio resources so as to minimize the cross-interference with pre-existing networks [34]: by distributed processing, nodes can cooperatively detect the *complete* interference patterns caused by active networks in the area, overcoming the limited sensing range at Host (or field device). Once resource scheduling has been performed and the cloud functionality has been set up, nodes can also perform distributed processing over the cloud platform to cooperatively monitor/control a common process: the cloud nodes are configured to gather and exchange local observations about the process state, augmenting the performance of their local sensors/actuators with the diversity gain and the extended coverage provided by the cloud ensemble.

In consensus-based distributed processing [23], the monitored parameters $\boldsymbol{\theta}$ (i.e., the interference level or any other variable of interest) is evaluated at each node i by computing an initial measure/estimate $\hat{\boldsymbol{\theta}}_i(0)$ from local measurements. The estimate is then refined based on iterated data exchange with neighbors, till a consensus is reached among the CNs, as shown in the example in Fig. 2-(c). To minimize inter-node signaling and guarantee convergence to the centralized system performance [23], a weighted-consensus strategy is considered where CNs exchange only parameter estimates (rather than raw data) using the pre-configured SBCH slots over consecutive super-frames. The update rule at node i and iteration $q = 1, 2, ...$ is as follows:

$$\hat{\boldsymbol{\theta}}_i(q+1) = \hat{\boldsymbol{\theta}}_i(q) + \varepsilon \mathbf{W}_i^{-1} \sum_{j \in \mathcal{N}_i} \left(\hat{\boldsymbol{\theta}}_j(q) - \hat{\boldsymbol{\theta}}_i(q) \right), \qquad (2)$$

where $\mathcal{N}_i$ denotes the set of neighbors for node i and $\mathbf{W}_i = \boldsymbol{\Gamma} \mathbf{C}_i^{-1}$ is a positive-definite weighting matrix that accounts for the reliability of the local observation, being $\mathbf{C}_i$ the covariance of $\hat{\boldsymbol{\theta}}_i(0)$ and $\boldsymbol{\Gamma}$ a scaling matrix. The step size ε is selected so as to guarantee convergence to the centralized solution $\hat{\boldsymbol{\theta}}_i(\infty) = \left(\sum_{j=1}^{N_S} \mathbf{C}_j^{-1} \right)^{-1} \sum_{i=1}^{N_S} \mathbf{C}_i^{-1} \hat{\boldsymbol{\theta}}_i$ (see [23] for details). Convergence is eased in dense cloud networks with high degree of connectivity. Experimental tests are presented in Sect. VI for distributed interference detection.

IV. Demonstration and measurement set-ups

In order to verify the performance of the proposed approaches, the validation of the test-bed occurred in two sites: the IdroLab facility, hosted in the ENEL (the largest Italian electric company) research and development center in Livorno, Italy and an oil&gas refinery site owned by PetroEcuador, the national oil company of Ecuador. A pictorial description of both sites is sketched in Fig. 4. The aim of the validation is to test the performance of the proposed wireless cloud platform and verify its ability to provide augmented services to the underlying IWSN system. Controlling the plant sites is thus out of the scope of these tests. For this reason, the wireless instruments adopted in the field tests are not actually attached to the plants, but they complement the legacy devices of existing wired process automation systems in order to experience similar harsh environmental conditions that would be not practical to reproduce by simulations.

In addition to the selected sites of Fig. 4, we have been able to collect a larger data-base of measurements in different industrial environments, although not specifically detailed in the paper. These additional experiments allowed to evaluate the performance of the proposed cloud functions under different propagation settings, ranging from short-range to propagation critical scenario as well as to perform a comparative analysis with a WirelessHART system, being the current de facto standard for process-control applications.

A. Testing sites

The IdroLab site is a pilot scale experimental plant purposely realized to test new technologies aimed at improving the efficiency and environmental impact of thermoelectric power generators [35]. The actual plant is split into two different sections: the hydraulic module (cool side, handling water re-circulation between two drums) and the thermal module (hot side, handling water evaporated in steam generator). The plant sections are located at different levels; on the mezzanine level there are the control room and the lower drum; the latter is connected by a centrifugal pump to the upper drum located on the first floor. The circulating pump and a reservoir tank are located on the ground level.

The 15.000 sqm Setria site inside the Esmeraldas oil&gas refinery has been chosen as an additional location for testing the consensus-based distributed sensing system over a large size open-area field. It consists of a section of an oil depot characterized by 6 large-size concrete fuel tanks. The industrial facility must ensure that the products are safely stored and handled (e.g. avoiding leakages), therefore revamping activities are currently planned by PetroEcuador to augment the existing monitoring and control systems. In this setting, wireless systems provide a cost-effective solution without the costly (and unfeasible for logistic reasons) re-wiring over the existing plant.

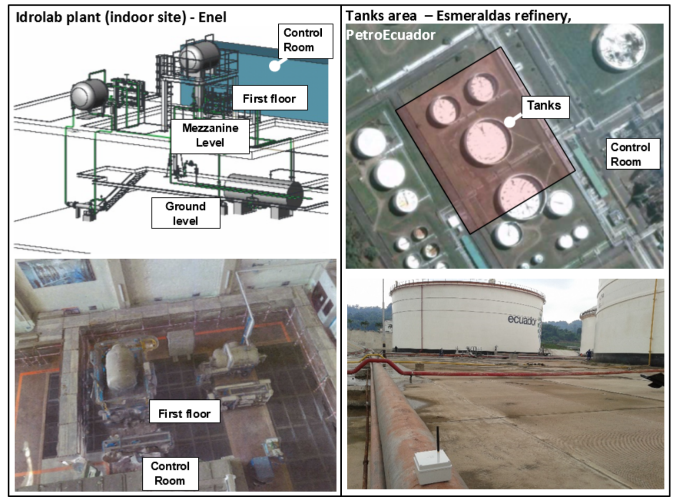

Fig. 4. Left: 3D layout of IdroLab plant (Enel, Italy): first floor, mezzanine level and ground floor. Right: Setria outdoor site (PetroEcuador Esmeraldas refinery, Ecuador).

B. Demonstration set-up

All the wireless devices deployed for the tests were battery powered. In our scenarios, the availability of standard 20Ah battery has been assumed (see Fig. 1): according to the available data, there is a clear evidence that the use of the cloud section, whose activation is based on specific requests, is convenient as reducing the consumption of the IWSN (offloading traffic to the cloud) in exchange for additional installed cloud devices. In order to set-up the cloud operations, the multi-hop chain sequence and sensing functions are configured separately for each test. For each setting, the deployment of CNs can be optimized either by on-site testing or based on 2D/3D model of the plant [10]. Each CN involved in data forwarding or distributed sensing will then automatically derive the applicable superframe configuration (see parameters in Fig. 3) from the selected chain sequence. This sequence configuration is also transmitted inside the data frame header from the CA node acting as source (as for typical source-routing schemes): this allows to make the routing path independent from the superframe configuration. Although the CN transceiver complies with the IEEE 802.15.4e PHY layer [36], it is configured to double the data-rate (to 500kb/s): this option ensures a substantial publishing rate increase while still guaranteeing an acceptable noise-immunity level (through DSSS implementation). The reduced DSSS spreading factor is counter-balanced by the hybrid multihop-cooperative transmission chain as well as the adoption of frequency hopping over consecutive virtual channels. For the purpose of spectrum sensing (Sect. VI), the CNs are equipped with an external single-chip spectrum analyzer (based on CC2511 [37]) with integrated frequency-synthesized tuning. The analyzer measures the power (Received Signal Strength, RSS) over the band $2.4 \div 2.485$GHz, with frequency step configured as $\Delta f = 333$kHz and sampling time (sweep time) $\Delta t = 536$ms. Power range is -110dBm to -6.5dBm, resolution 0.5dB.

V. CRITICAL DATA PUBLISHING

Current IWSN solutions based on TSCH mode [32] provide applications with limited scheduling options due to an optimized design for energy consumption and deterministic traffic management. As a result, some relevant mission-critical *data publishing* workloads required in specific industrial applications are more difficult (in some cases not possible) to handle. Data publishing happens when the field device detects some relevant conditions that might generally require either a low-latency reaction, a highly reliable or a high-throughput data transfer. In this section two critical process automation scenarios are identified which are not properly addressed by current IWSN implementations based on IEC 62591 standard.

The first scenario (Sect. V-A) is the *high-throughput datagram publishing*. It generally requires the cloud network to transfer a comparative large block of data from a source wireless node to a destination wireless node in the shortest possible time, where one of the nodes is generally located within a centralized supervising station. The typical application case is when a measurement field device sporadically collects a relatively large block of data to be transferred to a Host station (e.g. seismic/vibration measurement upload [38], waveform table transfer etc..) or when a block of data needs to be transferred to a field device to reprogram its operating mode (e.g. over-the-air firmware or software upgrade) for a modified application case. The performance indicator for this use case

Deployment (single floor) (a)

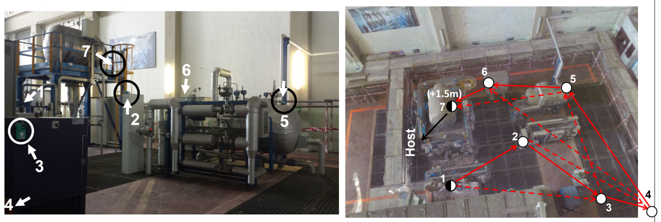

Performance indicators (Table 1)

	Packet Drop Rate PDR (CA node)	Max. link PER (direct and coop. links)	Datagram Throughput $TL/H \times \mathrm{P}(n)$	Co-channel Interference info.
#1 Route 1->7 (Tot. 18min)	1.1%	7% (link 1->2) 35% (link 5->7)	14.3 kb/s	WiFi (**inactive**), WirelessHART (**inactive**)
#2 Route 1->7 (Tot. 6min)	8.5%	15.7% (link 2->3) 26.8% (link 3->5)	13.2 kb/s	WiFi (**inactive**), WirelessHART (**active, joining phase**)
#3 Route 1->7 (Tot 20min)	1.0%	1.1% (link 2->3) 26% (link 3->5)	14.3 kb/s	WiFi (**inactive**), WirelessHART (**active**)
#4 Route 1->7 (Tot 6min)	3.5%	4.4% (link 6->7) 26% (link 3->5)	14.0 kb/s	WiFi (**active**), WirelessHART (**active**)

Deployment (3 floors) (b)

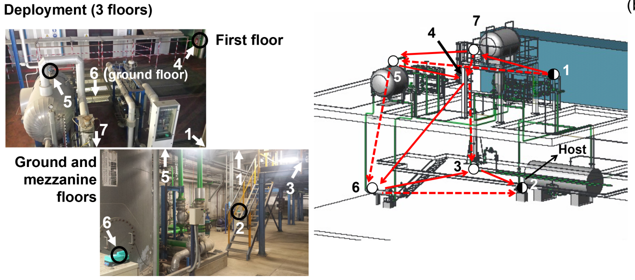

Performance indicators (Table 2)

	Packet Drop Rate PDR (CA node)	Max. Link PER (direct and coop. links)	Datagram Throughput $TL/H \times \mathrm{P}(n)$	Co-channel Interference info.
#5 Route 1,7,5,4,6,3,2 (Tot. 2 min)	3.2%	59% (link 4->5) 44.7% (link 4->6)	14.3 kb/s	WiFi (**active**), WirelessHART (**active**)
#6 Route 1,7,5,4,6,3,2 (Tot. 6 min)	8.5%	60% (link 4->5) 46.9% (link 2->4)	13.3 kb/s	WiFi (**2 networks active**), WirelessHART (**active**)
#7 Route 1,7,3,5,6,4,2 (Tot. 6 min)	2.9%	45.6% (link 5->6) 2.7% (link 3->5)	14.1 kb/s	WiFi (**1 network active**), WirelessHART (**active**)

Fig. 5. High throughput datagram publishing: selected results from the testing activity in IdroLab research plant. End-to-end PDR, max. link-level packet error rate (PER) for direct/cooperative links and datagram throughput (kb/s) are reported for each case. Images of the plant courtesy of ENEL.

is "datagram throughput" μ (kb/s). A substantial increase of the baseline datagram throughput should be made possible by the cloud section so that the overall reconfiguration time is minimized. The achievable throughput of current battery-powered IWSN based on TSCH mode is about 2-3 kb/s, and decreasing with the number of installed field devices. The desirable throughput should be instead increased up to 10 kb/s.

The second scenario (Sect. V-B) is the *low-latency publishing*. It requires the cloud network to handle asynchronous events taking place either at a remote wireless node or at the Host station (or both), so that suitable corrective actions can be applied. The performance indicator for this use case is therefore the latency (e.g., 95th percentile), measured with respect to the first successful datagram reception. Proper actuation/configuration actions should be typically characterized by a minimum delay, with desirable communication latency of 250 ms or below.

The availability of a low-latency "upstream" (field device to Host) and "downstream" (Host to field device) data forwarding mechanism also enables the fast exchange of request-response messages, consisting of one single – or at most a few – datagrams. For example, this service is required to support high-integrity configuration actions, where the Host needs to fully configure a new wireless device which has been added to the network according to the content of a pre-defined database located at the supervising station level. Given that each single configuration action needs to be sequential – i.e., the next configuration can proceed only after having received a "confirmation" response about the successful completion of the previous one – a "reliable" throughput measure can be adopted as performance indicator. This is obtained as the number of successful request-response messages (with payload $L = 80$ (B) bytes) per second, and here measured in kb/s.

In Fig. 5 results from the system validation in the IdroLab site are summarized. Latency results are then discussed in Fig. 6 by collecting measurements obtained in different environments ranging from short-range (Type I) to propagation-critical (or long-range, Type IV). Average performance figures for all scenarios are summarized in Fig. 7.

A. High-throughput datagram publishing

Fig. 5 summarizes the results for a scenario corresponding to the upstream publishing. For the tests, the cooperative chain system underlying the cloud connectivity is configured according to the *datagram transmission mode* (Sect. III-B). The hyper-frame (see Fig. 3) is therefore configured to support the transfer of a data-block between CN 1 acting as source and the Host-side CA (namely node 7 for tests #1-#4 and node 2 for tests #5,#6,#7), along with an end-to-end acknowledge about the transfer result. The hyper-frame is configured to carry $T \times L = 29 \times 80 = 2.3$kB of data ($T$ and L are defined in Fig. 3, on top) and has a duration of 16 super-frames (corresponding to $H = 1.28$s.). This choice allows the cloud network to transfer a meaningful block of data within a single hyper-frame being representative of a typical industrial scenario. Clearly, the hyper-frame size could be adapted so to fit the specific application in an optimal way. For all the tests, the effective achievable upstream throughput μ (kb/s) is measured as

$$\mu = \frac{T \times L}{H} \times \mathrm{P}(n), \tag{3}$$

with end-to-end packet drop rate (PDR), $1 - \mathrm{P}(n)$, and $\mathrm{P}(n)$ in (1).

Two deployments are highlighted, each consisting of 3-5 CNs and 2 CA nodes as an interface for field devices and Host station (through the TSCH interface). In the first scenario (tests #1-#4, Fig. 5-(a)) the cloud system is deployed on a single floor and covering a 120 sqm area. As target use case, the cooperative-multihop chain is deployed to connect the centrifugal pump section (node 1) with the upper drum (node 7) and the control room. The same tests also assessed possible co-existence issues with a WiFi network operating on 2.4GHz band (channel 1, test #4) and an additional interfering WirelessHART network (tests #2,#3). In the second setting

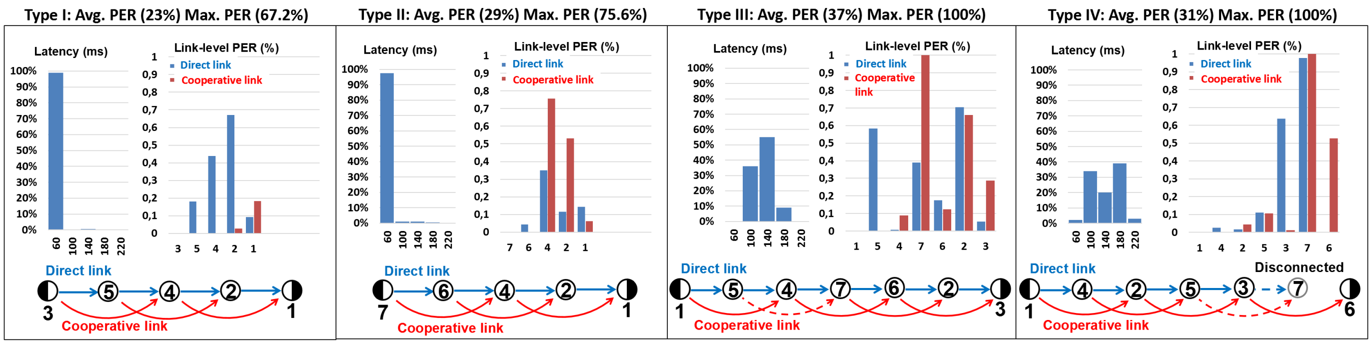

Fig. 6. Low latency publishing stress-test results under 4 different environments ranging from short-range (Type I) to propagation-critical (or long-range, Type IV). Probability mass function of the observed latency (ms), average, maximum and link-level PER are shown for each case; the corresponding chain topology is depicted below.

(tests #5-#6 and #7 in Fig. 5-(b)), the cloud system is now deployed over three different floors (ground, mezzanine and first floor), being representative of a typical harsh propagation scenario. In this case, the cloud enables a cooperative-multihop transmission chain that connects the control room with the ground level (reservoir tank, node 2). As shown in Table 1 and 2 of Fig. 5 typical interference signal features (e.g., consisting of one WiFi and one WirelessHART network publishing data on every 30s, see tests #3,#4,#5,#7) marginally affect the measured PDR. Instead, larger performance loss is observed in more critical scenarios featuring WirelessHART devices in joining state (with high duty cycle) and 2 WiFi networks spanning the full 2.4GHz band (tests #2,#6). Comparing the results obtained in a typical propagation scenario (Table 1) with those obtained in a more critical harsh propagation environment (Table 2) clearly shows that the joint use of the cooperative networking scheme for path redundancy together with frequency-hopping can balance signal distortions, caused by interference and multipath, being responsible of physical packet error rate (PER) up to 60% over many direct/cooperative links. In addition, as discussed in the next section, for these critical cases, the cloud platform can be configured to infer the specific interference patterns that are responsible for radio communication impairments.

A substantial increase of the baseline throughput μ with respect to current WirlessHART implementation is also shown as achievable by the proposed cloud platform. WirelessHART theoretical maximum link-layer throughput can be approximated as 10 data frames/s (or packets/s) corresponding to 6.4kb/s [2][39], and reduces in practical settings to 4 data frames/s (2.5kb/s) considering short multi-hop routes of 2 hops (typical) [32]. The datagram transmission mode, as supported by the cloud system, provides a theoretical max. figure of $\mu \leq \frac{T \times L}{H} = 14.5$kb/s and two-times larger throughput with respect to theoretical WirelessHART performance. Considering that the throughput in all the considered cases is $\mu > 12.8$kb/s, one order of magnitude increase could be therefore reasonably assumed as achievable in practical configurations.

		TSCH (WirelessHart)		Cloud platform (Cooperative-multihop)	
		3 hops	6 hops	3 hops	6 hops
High-throughput publishing	Datagram throughput (kb/s) – block transfer	2,5	2	14,5	13
Low-latency publishing	Reliable throughput (kb/s)	0.7	0.4	2.6	2.5
	95th percentile latency (ms)	180-250 (Typ. I-II)	260-500 (Typ. III-IV)	60-100 (Typ. I-II)	140-180 (Typ. III-IV)

Fig. 7. Comparative analysis with TSCH implementation in terms of high-throughput publishing (kb/s), and low latency publishing (reliable throughput - kb/s - and 95th percentile latency - ms).

B. Low-latency publishing and request-response

In this section the cloud network functions are now validated to support low-latency publishing and high-integrity request-response transactions. Given that both latency and reliability are key issues, a *reliable transmission mode* is chosen for the cooperative chain implementation (Sect. III-B). In Fig. 6 the experimental probability mass functions of the measured latency are collected from additional tests in four representative scenarios characterized by increasing propagation criticality. In particular in Type I scenario the multi-hop network is characterized by line-of-sight (LOS) short-range links, while Type IV is characterized by non line-of-sight (NLOS) long-range links and one CN (node 7) almost disconnected from the CA node (e.g., with RSS below the RX sensitivity). To allow for a comparative analysis with the experiments described in Fig. 5, link-level PER, as well as average and max. packet drop rate figures are also detailed for each scenario. 95th percentile latency is below 180ms in all cases, considering relatively short (3 hops) to long hopping sequences (6 hops). The use of the multihop-cooperative transmission chain provides a sufficiently high level of immunity to multipath fading and interference: it thus guarantees high reliability and a reasonable determinism of communication, being a crucial requirement for real-time control applications [40]. Compared to WirelessHART, typically showing a theoretical latency ranging from 300ms for short hopping chains (i.e., typically 3 hops),

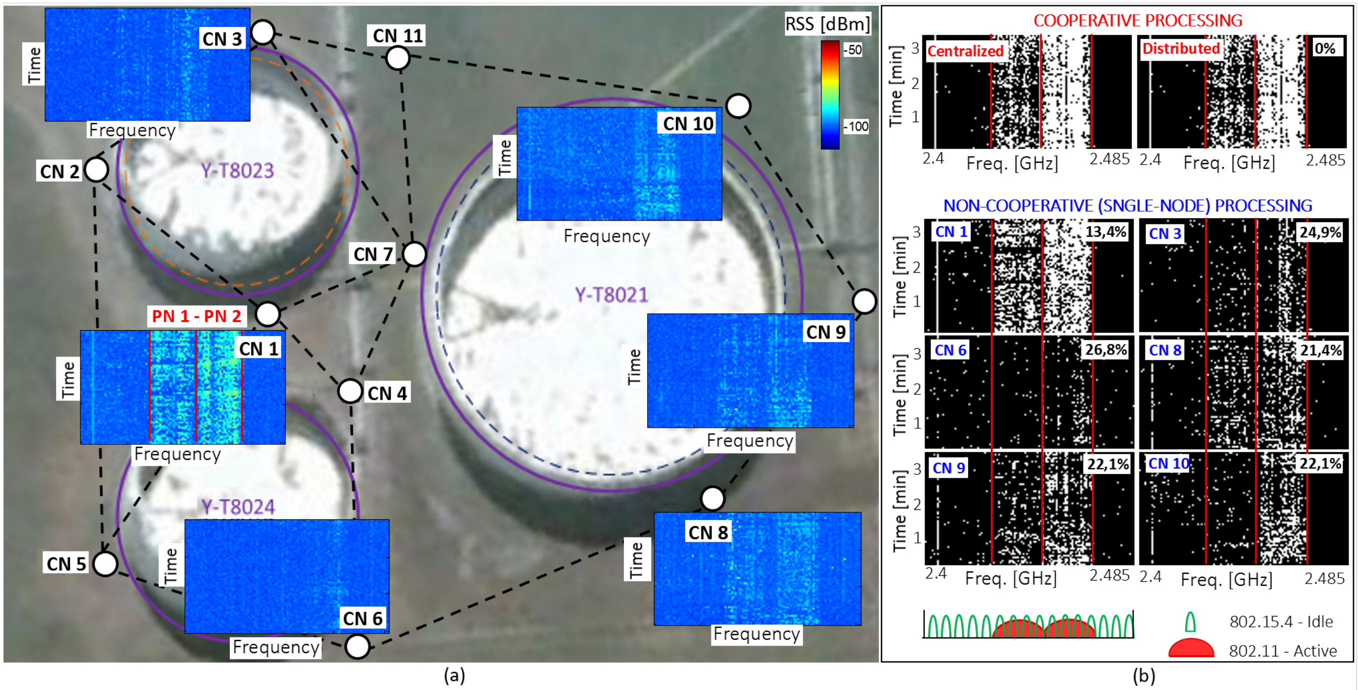

Fig. 8. Distributed sensing in PetroEcuador Esmeraldas refinery. (a) Spectrum sensing by $N_S = 11$ CNs collecting RSS measurements [dBm] over time and frequency. Two IEEE 802.11g PNs are transmitting in the same 2.4GHz band, as highlighted in the RSS data-set of CN 1. (b) Time-frequency interference maps detected by centralized (top-left) and distributed (top-right) cooperative algorithms, and by non-cooperative local processing at device CN i, $i = 1, 3, 6, 8, 9, 10$ (bottom). The probability of miss-classification is shown in the top-right corner of each sub-figure.

and up to 500ms-1s [32] for longer multi-hop sequences, the maximum publishing latency can be thus scaled down from 6 up to 10 times.

Current TSCH networks are typically able to lay in fast upstream/downstream bandwidth on a special graph known as the pipe: this is intended as a temporary addition to the network in order to handle the fast exchange of request-response messages. In the proposed system, the user can trigger this fast request-response exchange (e.g. for high-integrity configuration tasks) from the Host control station, and interfacing with the CA nodes – possibly for many devices at a time – with the need of completing it in the shortest possible time. Compared with typical TSCH pipe performance, the cloud platform is shown to provide three times larger reliable throughput, further improvements are expected when increasing the number of hops. The table in Fig. 7 considers all the tests and provides a summary of the achievable figures, focusing on high-throughput datagram transfer (kb/s), reliable throughput for request-response messages (kb/s) and corresponding 95th percentile latency (ms). For each case, the cloud platform performance is compared with current TSCH/WirelessHART implementation, for typical 3 to 6-hop topologies.

VI. Distributed Sensing for Autonomous Interference Learning

In the following experimental analysis, the cloud platform is exploited to support the *autonomous learning of interference patterns*: this use case is particularly critical in most of unlicensed spectrum sharing industrial applications [41]. In this case study, the Host station is configured to program the cloud SBCH channels (Fig. 2-(c)) to cooperatively identify the overall interference patterns caused by a pre-existing network of devices and forward the information to the network manager so to schedule TSCH resources over the unused portion of the spectrum and avoid mutual interference. Each cloud device might therefore retrieve partial estimates of frequency occupation (or time-frequency patterns) and share the information with neighbor devices based on consensus-based processing. The *local* knowledge about the TSCH *global* interference status allows each device to perform autonomous diagnostic and comparative performance tests.

Distributed sensing is analyzed in an experimental scenario where a pre-existing (primary) IEEE 802.11g network is active in the area of a cloud network and located inside the refinery control room (Fig. 4). The CNs have to sense the spectrum to detect the free regions where to allocate their own resources. As shown in Fig. 8-(a), the cloud is composed of $N_S = 11$ CNs, each having a partial visibility of the primary nodes (PN) interference due to limited radio range and obstructions caused by the tanks and other industrial equipment. The CNs engage in a distributed procedure to cooperatively identify the overall interference caused by the PNs. The set of the RSS measurements collected by the i-th CN can be defined in general as $\mathcal{X}_i = \{x_i(t, f)\}$, where (t, f) ranges over the time-frequency resources of the spectrum sensing instrument (Sect. III). The spectrum measurement data-sets are shown in Fig. 8-(a) for some selected devices: two PNs are interfering with the cloud, but some nodes can only sense one (e.g., CN 10) or none (CN 6). This motivates the employment of a distributed cooperative sensing strategy.

For interference detection, each RSS sample $x_i(t,f)$ is modeled, according to the log-normal power model, as a Gaussian random variable with parameters depending on the absence ($\mathcal{H}_0$) or presence ($\mathcal{H}_1$) of any interfering PN in (t,f): under hypothesis $\mathcal{H}_0$, with probability $1-P$, the RSS $x_i(t,f) \sim \mathcal{N}\left(\mu_0, \sigma_0^2\right)$ models the background noise power with mean μ_0 and variance σ_0^2; under hypothesis $\mathcal{H}_1$, with probability P, $x_i(t,f) \sim \mathcal{N}\left(\mu_1, \sigma_1^2\right)$ models the PN signal power received at CN i with mean $\mu_1 > \mu_0$ and variance $\sigma_1^2 > \sigma_0^2$ (due to shadowing effects).

For known interference statistics $\boldsymbol{\theta} = [\mu_1, \mu_0, \sigma_1^2, \sigma_0^2, P]^{\mathrm{T}}$, maximum-a-posteriori Bayesian detection of the interference activity can be implemented by comparing the RSS samples with the optimal threshold $S = S(\boldsymbol{\theta})$ resulting from the likelihood-ratio test [42]. However, the interference statistics $\boldsymbol{\theta}$ are unknown at the cloud. Also, to reconstruct the complete interference pattern from incomplete local data-sets, the cloud needs to aggregate all the RSS data $\mathcal{X} = \{x_i(t,f)\}$ from all nodes $i = 1,\ldots,N_S$ and time-frequency resources (t,f), which is typically unfeasible in self-organizing networks. We thus propose a consensus-based strategy [26] where the CNs distributedly aggregate the information, exchanging only compact detection data (rather than raw RSS) to minimize inter-node signaling. The method combines the weighted-consensus algorithm (2) with an iterative decision directed (DD) procedure [43] for joint estimation of the PN statistics $\boldsymbol{\theta}$ and detection of the interfered time-frequency resources associated with $\mathcal{H}_1$. Starting from an initial set $\hat{\boldsymbol{\theta}}^{(k)}$, at iteration $k = 0,1,2,\ldots$, interference detection is performed at each CN i using the threshold $\hat{S}^{(k)} = S(\hat{\boldsymbol{\theta}}^{(k)})$, and the local data $\mathcal{X}_i = \{x_i(t,f)\}$ is accordingly partitioned into two subsets associated to the hypotheses $\mathcal{H}_1$ and $\mathcal{H}_0$, $\mathcal{X}^{(k)}_{\mathcal{H}_1,i} = \{x \in \mathcal{X}_i : x \geq \hat{S}^{(k)}\}$ and $\mathcal{X}^{(k)}_{\mathcal{H}_0,i} = \mathcal{X}_i \setminus \mathcal{X}^{(k)}_{\mathcal{H}_1,i}$, respectively. New interference parameters are obtained by computing the sample means $(\hat{\mu}^{(k+1)}_{1,i}, \hat{\mu}^{(k+1)}_{0,i})$, variances $(\hat{\sigma}^{2(k+1)}_{1,i}, \hat{\sigma}^{2(k+1)}_{0,i})$ and frequencies $(\hat{P}^{(k+1)}_i = |\mathcal{X}^{(k)}_{\mathcal{H}_1,i}|/|\mathcal{X}_i|)$ for the subsets $\mathcal{X}^{(k)}_{\mathcal{H}_1,i}$, $\mathcal{X}^{(k)}_{\mathcal{H}_0,i}$. A number of consensus iterations (2) is then performed to fuse the estimates at different CNs and get the new interference statistics $\hat{\boldsymbol{\theta}}^{(k+1)}$ as virtually obtained by the aggregation of $\{\mathcal{X}^{(k)}_{\mathcal{H}_0,i}, \mathcal{X}^{(k)}_{\mathcal{H}_1,i}\}_{i=1}^{N_S}$ over the whole cloud. The DD method is repeated till convergence when $\hat{P}^{(k)}_i = \hat{P}^{(k+1)}_i = \hat{P}^{(\infty)}_i$.

Fig. 8-(b) shows the binary masks obtained by distributed detection of the time-frequency interference patterns caused by the IEEE 802.11g primary networks. Binary masks are evaluated for both cooperative and non-cooperative (single-node) algorithms. The probability of miss-classification, defined as the percentage of the errors with respect to the centralized approach (here considered as reference), is indicated for all methods. It can be seen that non-cooperative detection is highly affected by errors due to partial visibility and signal blockage, while the distributed method based on weighted-consensus significantly outperforms the non-cooperative one reaching the centralized detection performance.

VII. Conclusions

In this paper we developed an hardware and software architecture for integrating a cloud network system with an industrial wireless sensor network compliant with the TSCH network mode and WirelessHART standard (IEC 62591). A novel field-level cooperative forwarding scheme was validated to efficiently address critical data publishing services that require fast transfer of data under stringent throughput, reliability and latency constraints. Low-level cooperation of cloud devices was also harnessed to implement consensus-based distributed sensing functions that are provided as a service for upper-level network managing tasks. These cloud functions were validated for on-demand autonomous identification of recurring interference patterns. The cloud demonstrator was tested in two representative industrial sites. Experimental activities were carried out to demonstrate the feasibility and the effectiveness of the proposed system, and highlighted the potential of the technology as compared with current industry-standard wireless solutions.

Acknowledgment

The authors would like to thank the ENEL, PetroEcuador and ESPOL personnel for hosting the experimental activities inside the IdroLab plant and the Esmeraldas refinery site, respectively and for all the fruitful discussions.

References

[1] M. R. Palattella, M. Dohler, A. Grieco, G. Rizzo, J. Torsner, T. Engerl, L. Ladid, “Internet of Things in the 5G era: enablers, architecture, and business models,” IEEE J. on Selected Areas in Communications, vol. 34, no. 3, Mar. 2016.

[2] S. Petersen, S. Carlsen, “WirelessHART versus ISA100.11a: the format war hits the factory floor,” IEEE Ind. Electronics Mag., vol. 5, no. 4, pp. 23-34, Dec. 2011.

[3] A. Flammini, E. Sisinni, “Wireless sensor networking in the Internet of Things and cloud computing era,” Procedia Engineering - the 28th European Conference on Solid-State Transducers, EUROSENSOR 2014, vol. 87, pp. 672-679, Brescia, Italy, Sep. 2014, DOI 10.1016/j.proeng.2014.11.577.

[4] M. Fazio, A. Puliafito, “Cloud4sens: a cloud-based architecture for sensor controlling and monitoring,” IEEE Communications Magazine, vol. 53, no. 3, pp. 41-47, Mar. 2015.

[5] A. Alamri, W. S. Ansari, M. M. Hassan, M. S. Hossain, A. Alelaiwi, and M. A. Hossain, “A survey on sensor-cloud: architecture, applications, and approaches,” International Journal of Distributed Sensor Networks, vol. 2013, Article ID 917923, 18 pp., 2013.

[6] Y. Lim and J. Park, “Sensor Resource Sharing Approaches in Sensor-Cloud Infrastructure,” International Journal of Distributed Sensor Networks, vol. 2014, Article ID 476090, 8 pp., 2014.

[7] D. Zuehlke, “Smart factory - towards a factory-of-things,” Annual Reviews in Control, vol. 34, no. 1, pp. 129-138, Apr. 2010.

[8] L. D. Xu, W. He and S. Li, “Internet of Things in Industries: a survey,” IEEE Trans. in Industrial Informatics, vol. 10, no. 4, pp. 2233-2243, Nov. 2014.

[9] O. Givehchi, H. Trsek and J. Jasperneite, “Cloud computing for industrial automation systems — a comprehensive overview,” Proc. of IEEE 18th Conference on Emerging Technologies & Factory Automation (ETFA), Cagliari, 2013.

[10] S. Savazzi, V. Rampa, U. Spagnolini “Wireless cloud networks for the Factory of Things: connectivity modeling and layout design,” IEEE Internet of Things Journal, vol. 1, no. 2, pp. 180-195, Apr. 2014.

[11] V. C. Gungor and G. P. Hancke, “Industrial Wireless Sensor Networks: Challenges, Design Principles, and Technical Approaches,” IEEE Transactions on Industrial Electronics, vol. 56, no. 10, pp. 4258-4265, Oct. 2009.

[12] T. Rault, A. Bouabdallah, Y. Challal, “Energy efficiency in wireless sensor networks: a top-down survey,” Computer Networks, vol. 67, no. 4, pp. 104-122, July 2014, ISSN 1389-1286.

[13] P. Suriyachai, U. Roedig, A. Scott, “A survey of MAC protocols for mission-critical applications in wireless sensor networks,” IEEE Communications Surveys & Tutorials, vol. 14, no. 2, 2012.

[14] W. Shen, T. Zhang, F. Barac, M. Gidlund, “PriorityMAC: a priority-enhanced MAC protocol for critical traffic in industrial wireless sensor and actuator networks,” IEEE Trans. on Industrial Informatics, vol. 10, no. 1, Feb. 2014.

[15] T. Zheng, M. Gidlund and J. Åkerberg, “WirArb: a new MAC protocol for time critical industrial wireless sensor network applications,” IEEE Sensors Journal, vol. 16, no. 7, pp. 2127-2139, April, 2016.

[16] I. Khan, F. Belqasmi, R. Glitho, N. Crespi, M. Morrow and P. Polakos, “Wireless sensor network virtualization: a survey,” IEEE Communications Surveys & Tutorials, vol. 18, no. 1, pp. 553-576, 2016.

[17] S. Ma, Y. Yang and H. Sharif, “Distributed MIMO technologies in cooperative wireless networks,” IEEE Communications Magazine, vol. 49, no. 5, pp. 78-82, May 2011.

[18] X. Tao, X. Xu and Q. Cui, “An overview of cooperative communications,” IEEE Commun. Mag., vol. 50, no. 6, pp. 65-71, 2012.

[19] S. Savazzi, U. Spagnolini, “Distributed orthogonal space-time coding: design and outage analysis for randomized cooperation,” IEEE Trans. on Wireless Communications, vol. 6, no. 12, pp. 4546-4557, Dec. 2007.

[20] P. Castiglione, S. Savazzi, M. Nicoli, T. Zemen, “Impact of fading statistics on partner selection in indoor-to-outdoor cooperative networks,” Proc. of the IEEE International Conference on Communication ICC, Cape Town, South Africa, 23-27 May 2010.

[21] N. Marchenko, T. Andre, G. Brandner, W. Masood, C. Bettstetter, “An experimental study of selective cooperative relaying in industrial wireless sensor networks,” IEEE Trans. on Industrial Informatics, vol. 10, no. 3, Aug. 2014.

[22] S. Savazzi, “Wireless virtual multiple antenna networks for critical process control: protocol design and experiments,” International Journal of Distributed Sensor Networks, vol. 2013, Article ID 973621, 15 pages, 2013. doi:10.1155/2013/973621.

[23] M. Nicoli, G. Soatti, S. Savazzi, “Distributed estimation of macroscopic channel parameters in dense cooperative wireless networks,” Proc. of the IEEE Wireless Communications and Networking Conference (WCNC), pp. 972-977, Apr. 2014.

[24] M. A. Alvarez, B. Azari, and U. Spagnolini, “Time and frequency self-synchronization in dense cooperative networks,” Proc. of the IEEE Asilomar Conference on Signals, Systems, and Computers (ACSSC), pp. 1811-1815, Nov. 2014.

[25] G. Soatti, M. Nicoli, A. Matera, S. Schiaroli, U. Spagnolini, “Weighted consensus algorithms for distributed localization in cooperative wireless networks,” Proc. of the IEEE Int. Symposium on Wireless Commun. Systems (ISWCS), pp. 116-120, Aug. 2014.

[26] G. Soatti, M. Nicoli, S. Savazzi, U. Spagnolini, “Distributed sensing of interference pattern in dense cooperative wireless networks,” Proc. of the IEEE International Conference on Communications (ICC), pp. 961 - 966, Jun. 2015.

[27] L. Chen, G. Carpenter, S. Greenberg, J. Frolik, and X. S. Wang, “An implementation of decentralized consensus building in sensor networks,” IEEE Sensors Journal, vol. 11, no. 3, pp. 667-675, Mar. 2011.

[28] V. Jeličić, D. Tolić, and V. Bilas, “Consensus-based decentralized resource sharing between co-located Wireless Sensor Networks,” Proc. of the IEEE Ninth International Conference on Intelligent Sensors, Sensor Networks and Information Processing (ISSNIP), Singapore, pp. 1-6, Apr. 2014.

[29] J. Sýkora and H. Mark, “Dense cooperative wireless cloud network (DIWINE)”, Proc.s of the Future Network and Mobile Summit (FuNeMS), 3-5 Jul. 2013.

[30] R. Olfati-Saber, J. A. Fax, R. M. Murray, “Consensus and cooperation in networked multiagent systems,” Proc. of the IEEE, vol. 95, no. 1, pp. 215-233, Jan. 2007.

[31] Atmel, ATmega256RFR2, 8-bit AVR microcontroller with low-power 2.4GHz transceiver for ZigBee and IEEE 802.15.4, Revision B, Feb. 2013.

[32] Standard IEC 62591:2010, Industrial communication networks - Wireless communication network and communication profiles - WirelessHART™, Edition 2.0, 06 Nov. 2015.

[33] L. Pei, T. Zhifeng, S. Narayanan, T. Korakis, S. S. Panwar, “CoopMAC: A cooperative MAC for wireless LANs,” IEEE Journal on Selected Areas in Communications, vol. 25, no. 2, pp. 340-354, Feb. 2007.

[34] S. Mishra, A. Sahai, R. Brodersen, “Cooperative sensing among cognitive radios,” Proc. of the IEEE International Conference on Communications (ICC), pp. 1658-1663, Jun. 2006.

[35] P. Zand, E. Mathews, P. Havinga, S. Stojanovski, E. Sisinni, P. Ferrari, “Implementation of WirelessHART in the NS-2 simulator and validation of its correctness,” Sensors, vol. 14, no. 5, pp. 8633-8668, May 2014.

[36] IEEE Standard for Local and metropolitan area networks - Part 15.4: Low-rate wireless personal area networks (LR-WPANs) amendment 1: MAC sublayer, IEEE Std 802.15.4e™-2012, Apr. 2012.

[37] Texas Instruments, Low-Power SoC (System-on-Chip) with MCU, memory, 2.4 GHz RF Transceiver, and USB (Rev. G) CC2510Fx, CC2511Fx, (Rev. D), 2016.

[38] S. Savazzi, U. Spagnolini, L. Goratti, D. Molteni, M. Latva-aho, M. Nicoli , “Ultra-Wide band sensor networks in oil and gas explorations,” IEEE Communcations Magazine, vol. 51, n. 4, pp. 142-153, Apr. 2013

[39] P. Ferrari, A. Flammini, M. Rizzi, E. Sisinni, “Improving simulation of wireless networked control systems based on WirelessHART,” Computer Standards & Interfaces, vol. 35, no. 6, pp. 605-615, Nov. 2013. DOI 10.1016/j.csi.2013.04.003.

[40] A. Willig, “Recent and emerging topics in wireless industrial communications: a selection,” IEEE Transactions on Industrial Informatics, vol. 4, no. 2, pp. 102–124, May 2008.

[41] F. Barac, S. Caiola, M. Gidlund, E. Sisinni, T. Zhang, “Channel diagnostics for wireless sensor networks in harsh industrial environments,” IEEE Sensors Journal, vol. 14, no. 11, pp. 3983-3995, Nov. 2014.

[42] A. D. Whalen, Detection of signal noise, Academic Press, 1971.

[43] U. Spagnolini, “Cancellation of polarized impulsive noise using an azimuth-dependent conditional mean estimator,” IEEE Trans. Signal Processing, vol. 46, pp. 3333-3344, Dec. 1998.